engineering proceedings

MDPI

Proceeding Paper

Specific Aspects of Modelling Heat and Mass Transfer During Condensed Phase Precipitation on Heat Exchanger Walls †

Illia Petukhov, Oleksii Lysytsia *, Taras Mykhailenko and Artem Kovalov

Faculty of Aviation Engines, Aerospace Thermal Engineering Department Kharkiv, National Aerospace University "Kharkiv Aviation Institute", 61070 Kharkiv, Ukraine; i.petukhov@khai.edu (I.P.); t.mykhailenko@khai.edu (T.M.); a.kovalov@khai.edu (A.K.)

* Correspondence: a.lisitsa@khai.edu

† Presented at the 14th EASN International Conference on "Innovation in Aviation & Space towards sustainability today & tomorrow", Thessaloniki, Greece, 8–11 October 2024.

Abstract: When the vapour–gas mixture flow heats the cold walls of a heat exchanger, condensed phase (solid and liquid) precipitation can occur on their surfaces. This study aims to improve a model of thermohydraulic processes in a heat exchanger during condensed phase precipitation on its cold surfaces. The process is considered to occur when a multi-component solid-phase layer and a liquid film are simultaneously formed on the wall. Heat is transferred to the interface surface through radiation and convection and due to the phase transition of diffusing components. The mass flow to the interphase surface is determined for each diffusing component. The developed model allows for the calculation of heat transfer parameters in both steady-state and transient conditions, taking into account the formation of a multi-component condensed phase on cold walls.

Keywords: condensation; icing process; diffusing components; hydrogen; heat exchanger

check for updates

Academic Editors: Spiros Pantelakis, Andreas Strohmayer and Nikolaos Michailidis

Published: 27 March 2025

Citation: Petukhov, I.; Lysytsia, O.; Mykhailenko, T.; Kovalov, A. Specific Aspects of Modelling Heat and Mass Transfer During Condensed Phase Precipitation on Heat Exchanger Walls. *Eng. Proc.* **2025**, *90*, 84. https://doi.org/10.3390/engproc2025090084

Copyright: © 2025 by the authors. Licensee MDPI, Basel, Switzerland. This article is an open access article distributed under the terms and conditions of the Creative Commons Attribution (CC BY) license (https://creativecommons.org/licenses/by/4.0/).

1. Introduction

When the vapour–gas mixture flow heats the cold walls of a heat exchanger, a condensed phase (solid and liquid) may precipitate on these walls. Such conditions can occur in the fuel supply system of a hydrogen aircraft engine. In the case of liquid hydrogen (LH2) heating by exhaust gas, not only H_2O, but also N_2, O_2, etc., can precipitate on the heat transfer surface. As a result, the roughness and thermal resistance of the heat exchanger walls increase, and the cross-section of the vapour–gas mixture flow decreases. In critical cases, solid-phase crystals can even damage structural elements.

Heat and mass transfer processes, which occur during condensation and the subsequent crystallisation of moisture on supercooled surfaces, were examined in studies [1–4], focusing on aircraft icing issues. The Navier–Stokes equations of a viscous compressible gas were used in these studies to calculate the airflow parameters. The authors of [5] incorporated various models of heterogeneous media mechanics for droplet movement. Nevertheless, insufficient attention is paid to the heat exchange processes near a cold surface.

Film condensation is a common phenomenon in phase change heat transfer. Experiments on R134a vapour condensation on the cooled horizontal tube are presented in [6]. A theoretical study on the condensed film flow on a horizontal pipe with suction effects on the surface is presented in [7]. A lot of attention is paid to condensation issues, including heat and mass transfer during condensation in the presence of a noncondensable gas [8,9] and atmospheric water vapour condensation on surfaces [10]. Here, water vapour is usually

in the condensing phase, and the subsequent crystallisation of moisture is not considered. There are practically no studies on the condensation of N_2, O_2, etc.

Both classical approaches [11,12] and the relationships obtained based on modern experiments [13,14] are used to describe a coupled heat transfer process. However, there is no single and generally accepted approach to model thermohydraulic processes during condensation and the crystallisation of the condensed phase on the heat exchanger walls. While cryogenic heat exchangers are typical components of the aircraft fuel system [15], hydrogen liquefaction plants [16], and industrial installations [17], the questions of condensed phase formation and the icing of surfaces as a result of cryogenic liquid heating are not sufficiently studied and require further research.

2. Methodology

This study aims to improve a model of thermohydraulic processes in the heat exchanger during condensed phase precipitation on its cold surfaces. The process under analysis foresees a simultaneous formation of a multi-component solid-phase layer and a liquid film on the walls' surfaces. The ice structure and composition can vary significantly through the thickness because of the different thermophysical properties of the diffusing components. The desublimation process of a specific component is completed when the interphase surface temperature reaches the component's melting temperature. Subsequently, the crystallisation process engages components with higher triple-point temperature crystallisation, while others form a liquid film.

As a general case, a thermally insulated hydrogen pipeline (Wall 2 in Figure 1) with an external moisture-proof casing (Wall 1) can be considered. The annular space between them is filled with thermal insulation. On the outer side, there is a solid layer phase, "S" (the temperature zone below the melting point of the diffusing component), and a liquid film, "L" (the temperature zone above the melting point of the diffusing component). The film thickness is determined by the adhesive properties and viscosity of the diffused component and by the gravity and shear forces at the interface with the gas mixture flow. Index "g" marks the components of the mixture whose contribution to the condensation process at the temperature of the interfacial surface Tσ can be neglected. Other diffusing components are indicated by "v".

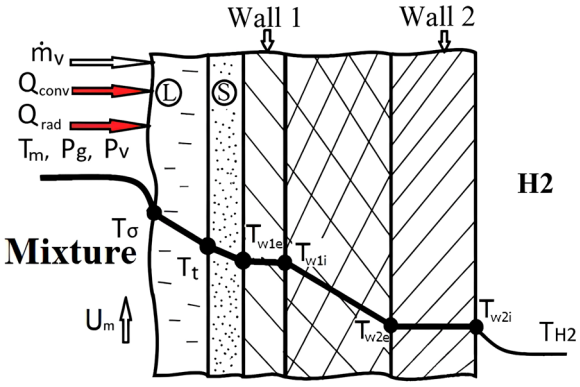


Figure 1. Heat flux scheme for thermally insulated hydrogen pipeline.

The temperature T_σ at the interface with the gas mixture flow is determined from the heat balance equation, which can be written as

$$Q_{ph} = Q_{ht} - (Q_{conv} + Q_{rad}) \quad (1)$$

The equation describes the fact that the algebraic sum of heat flux to the interfacial surface is equal to the heat flux Q_{ph} spent on the phase transition. Heat flux is transferred to

this boundary by radiation Q_{rad} and convection Q_{conv} and due to the phase transition heat of the mass flow $\dot{m}_{Vj}$ by diffusing components (Figure 1). The heat flux Q_{ht} corresponds to the heat removed from the phase transition surface to the hydrogen flow through the multi-layer cylindrical wall with the calculated heat transfer coefficient from the hydrogen side.

As the interphase surface temperature increases, the diffusion flow of each component decreases. The diffusion flow stops entirely when the vapour density of the diffusing component in the mixture flow and on the interphase surface becomes equal. Another factor influencing the formation of a condensed layer is the aggregate state of the condensed component, which depends on its triple point temperature. Initially, a liquid film of condensate forms on the surface of a growing ice layer from a diffusing component with the lowest triple-point temperature. This film can prevent other, more refractory diffusing components from agglomerating with this layer. Additionally, the aerodynamic interaction between the liquid film and adjacent gas flow can change the surface shape [1]. In this case, the appearance of a sludge-like medium that breaks down into a gas flow is possible.

The icing process can be modelled in both stationary and non-stationary formulations. In the stationary case, where the parameters of hydrogen and mixture flows are fixed, the thickness and structure of the condensed layer and the corresponding temperature profile along the radius are determined. It should be noted that the maximum ice thickness corresponds to the condition of the liquid film's formation on its surface. The process of desublimation without changing the temperature of the interphase surface Tσ is replaced by the process of condensation with a corresponding decrease in the heat of the phase transition and diffusion heat flux. This aspect shall also be taken into account when modelling the ice growth process.

The mathematical model used for calculating ice formation is based on the heat balance equation shown in (1). This equation defines the heat flux resulting from the phase transition of the diffused components from the vapour state at the temperature of the mixture (enthalpy h_{Vj}; mass flow rate $\dot{m}_{Vj}$) to the condensed phase's solid or liquid state at the boundary temperature T_σ (enthalpy $h_{\sigma j}$), which is defined as

$$Q_{ph} = \sum_{j=1}^{n} \dot{m}_{Vj}(h_{Vj} - h_{\sigma j}) \quad (2)$$

The enthalpy difference in component j in (2) can be defined as

$$h_{Vj} - h_{\sigma j} = L_{ivj}(T_\sigma) + c_{pVj}(T_m - T_\sigma) \quad (3)$$

where c_{pVj} is the heat capacity of a gaseous component, and T_m is the mixture temperature. The phase transition heat L_{ivj} is determined considering the aggregation state of the condensed layer on the wall. The phase transition heat here has a decisive contribution.

Convective heat flux from the mixture side is defined as

$$Q_{conv} = h_{cm}(T_m - T_\sigma)\pi d_\sigma L \quad (4)$$

Heat transfer coefficient (HTC) h_{cm} in (4) is determined using the criterion equations, which have following forms for the case of transverse flow around a single pipe [13]:

$$Re < 10^3 \; Nu = 0.56 Re^{0.5} \, Pr^{0.36} \left(\frac{Pr_m}{Pr_\sigma}\right)^{0.25} \quad (5)$$

$$Re > 10^3 \; Nu = 0.28 Re^{0.6} \, Pr^{0.36} \left(\frac{Pr_m}{Pr_\sigma}\right)^{0.25} \quad (6)$$

Heat flux Q_{ht} corresponds to the heat removed from the phase transition surface to the hydrogen flow,

$$Q_{ht} = h_{ht}(T_\sigma - T_{H2})\pi L \quad (7)$$

where h_{ht} is a linear heat transfer coefficient that is calculated for a multi-layer cylindrical pipe model, T_{H2} is hydrogen temperature, and L is the length of the heat exchanger section.

The mass flow to the interphase surface $\dot{m}_{Vj}$ is determined by the mass transfer equation, which has the following form for each of the diffusing components:

$$\dot{m}_{Vj} = h_{Dj}\pi d_\sigma L(\rho_{vj} - \rho_{v\sigma j}) \quad (8)$$

where h_{Dj} is a mass transfer coefficient, and ρ_{vj} and $\rho_{v\sigma j}$ are the vapour densities of the diffusing component in the mixture flow and on the interphase surface, respectively.

Within the quasi-equilibrium phase transition framework [13,14], the vapour phase and the condensed phase on the interphase surface are assumed to be in thermodynamic equilibrium. Therefore, the density of the vapour phase corresponds to the saturation state at temperature T_σ. Assuming the analogy of heat and mass transfer processes [13,14], the coefficient h_{Dj} can be calculated using the criterion equations in the following forms:

$$Re < 10^3\ Nu_{Dj} = 0.56Re^{0.5}\ Sc_j^{0.36} \quad (9)$$

$$Re > 10^3\ Nu_{Dj} = 0.28Re^{0.6}\ Sc_j^{0.36} \quad (10)$$

The mass flow to the interfacial surface determines the growth rate of the ice layer,

$$dr_\sigma/dt = \frac{1}{\pi L d_\sigma}\sum_{j=1}^{k}\frac{\dot{m}_{Vj}}{\alpha_{sj}\,\rho_{sj}} \quad (11)$$

where d_σ is an interfacial surface diameter, and α_{sj} and ρ_{sj} are the volume fraction and density of the component in the solid state, respectively.

The difference in the properties of the diffusing components and their fraction in the gas mixture determines the change in the mass flow of each of them when the temperature of the interphase surface changes. During the initial stage, all diffusing components may be presented in the ice layer. The mass fraction of each of them is determined by the following relation:

$$Y_j = \dot{m}_{Vj} \Big/ \sum_{j=1}^{k}\dot{m}_{Vj} \quad (12)$$

The corresponding volume fraction, taking into account the effective density of the solidified component, can be determined as

$$\alpha_j = \left(\frac{\dot{m}_{Vj}}{\alpha_{sj}\,\rho_{sj}}\right) \Big/ \sum_{j=1}^{k}\frac{\dot{m}_{Vj}}{\alpha_{sj}\,\rho_{sj}} \quad (13)$$

It is important to note that no experimental data corresponding to these study conditions could be found in the literature. In this regard, the model was verified by comparing the calculated results with specific data obtained during hydrogen heat exchanger testing within the Tu-155 Program [18]. The heat exchanger was located in the engine nozzle and was blown by a flow of hot exhaust gas. The average ice thickness over the heat exchanger surface was chosen as a comparison criterion. The difference between the calculated and experimental data did not exceed 30%. The validity of the approach used to model the

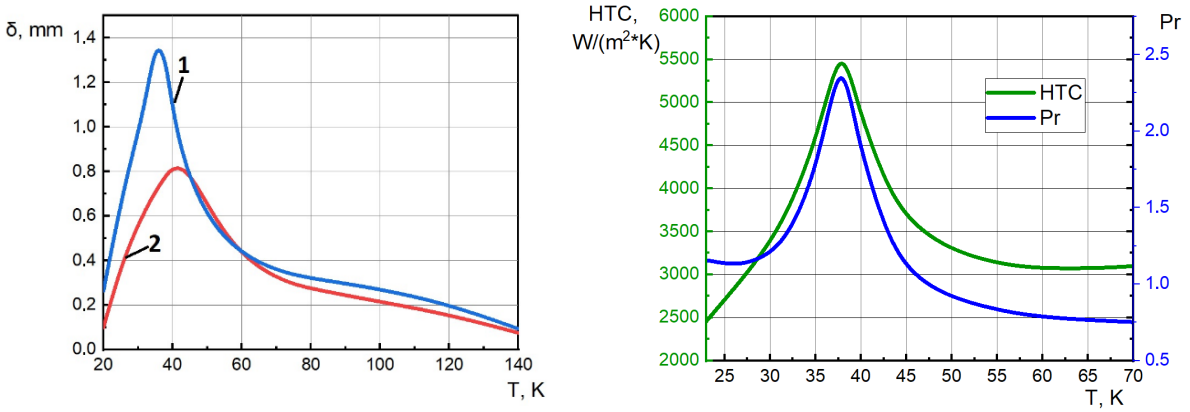
diffusion flow is confirmed by its widespread use for describing the processes of moisture condensation from steam–gas mixtures [11,12,19].

3. Results and Discussion

The influence of various factors on the icing process was studied by using the developed model. Key factors included the tube diameter, the temperature, pressure and flow rate of hydrogen, and the temperature, composition, and pressure of the adjacent hot flow. Calculations were carried out for humid air and exhaust gas, with hydrogen parameters corresponding to various engine operating modes.

For the water ice layer to grow, the temperature of the interfacial surface T_σ must remain below 273.15 K, provided that the heat flux Q_{ht} is removed (to hydrogen). The heat flux Q_{ht} exceeds the heat flux to the interfacial surface, which also includes the diffusion flux Q_{ph} (1) during the desublimation of water vapour. These conditions depend on not only the temperature and the flow rate of hydrogen, but also on a set of thermophysical properties that determine the heat transfer coefficient from hydrogen. The maximum ice thickness corresponds to the condition, where a liquid film begins to form on its surface at the same temperature of 273.15 K. In this case, the diffusion heat flux Q_{ph} is determined by the heat of condensation, which is lower than the heat of desublimation.

The HTC from hydrogen has a significant influence on the ice formation process, considering, for example, a nonmonotonic relationship between the ice thickness and hydrogen temperature (Figure 2a). Moreover, in the stationary mode, the ice thickness even increases when increasing the H2 temperatures within the range of 23–39 K. For an H2 flow rate of 10 g/s, the maximum HTC is approximately 5500 W/(m^2 K) (Figure 2b) at a temperature of 38 K, which corresponds to the maximum ice thickness (Figure 2a, curve 1).

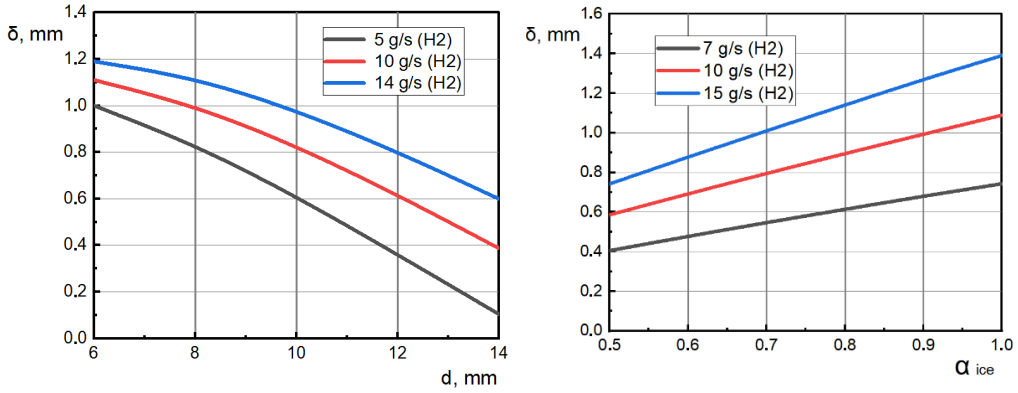


(**a**) (**b**)

Figure 2. Dependencies of (**a**) ice thickness and (**b**) heat transfer coefficient and Prandtl number (hydrogen side) on hydrogen temperature for hydrogen flow rate of 10 g/s, P = 20 bar, and exhaust gas temperature of 665 K. Tube inner diameter is 10 mm, and wall thickness is 1 mm; 1—hydrogen pressure 20 bar; 2—hydrogen pressure 40 bar.

In this case, a complex nature of the HTC variation is associated exclusively with the nonmonotonic temperature dependence of the thermophysical properties in the near critical region (33 K, 13 bar) for hydrogen. This behaviour is also reflected in the temperature dependence of the Prandtl number (Figure 2b). Additionally, for the analysed conditions, the Reynolds number increases significantly when the hydrogen temperature increases within the range of 23–39 K. Exhaust gas with a temperature of 665 K and a pressure of 0.41 bar at a speed of 290 m/s is used as a hot coolant.

As the hydrogen pressure increases, the influence of the critical point becomes less pronounced. However, the nonmonotonic relationship between the ice layer thickness and temperature persists (Figure 2a). This fact highlights the importance of accurately describing hydrogen's thermophysical properties, even for the single-phase states. In a steady mode, at fixed temperature and hydrogen pressure, the water ice layer thickness decreases as the hydrogen flow rate decreases and the tube diameter increases (Figure 3a). This is due to the HTC decreasing with the decrease in the Reynolds number. The relationship between the ice thickness and the ice porosity is shown in Figure 3b.



(**a**) (**b**)

Figure 3. Dependencies of (**a**) ice thickness on pipe diameter and (**b**) ice thickness on porosity of its structure for different hydrogen mass flow rates. Coolant—hydrogen at temperature of 40 K and pressure of 40 bar; exhaust gas temperature is 665 K. Tube inner diameter is 10 mm; wall thickness is 1 mm.

Humid air at ISO settings has a significantly lower temperature, resulting in a much greater maximum ice layer thickness for the same tube without thermal insulation. For example, for an H2 mass flow rate of 10 g/s, the ice layer may be 13 mm thick.

In transient processes, the thickness and structure of the ice layer change over time, leading to a corresponding change in temperature field and heat fluxes. Preliminary estimates show that the change in the enthalpy of structural materials due to the temperature field variation is negligible compared to the one that determines the ice layer formation. The dynamics of ice growth for three different H2 flow rates is presented in Figure 4.

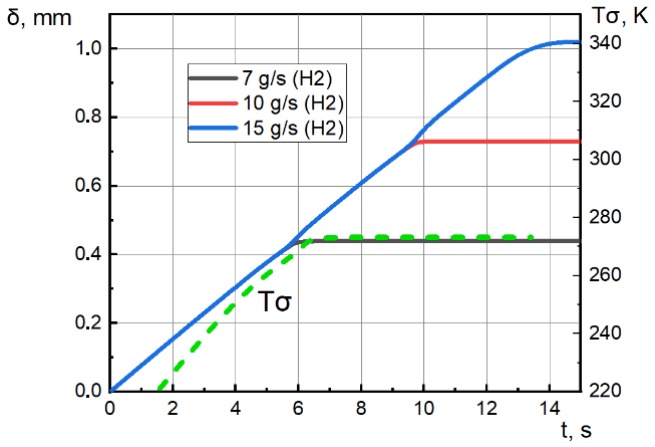


Figure 4. Dynamics of ice formation for different H2 mass flow rates. Coolant—hydrogen at T = 40 K and P = 40 bar; temperature of exhaust gas is 665 K. Tube inner diameter is 10 mm; wall thickness is 1 mm.

The maximum ice thickness depends significantly on the operation mode as the heat transfer coefficient depends on the hydrogen velocity. At the same time, the ice growth rate remains almost constant. This is primarily due to a very low density of water vapour on the interfacial surface. Consequently, the density difference, which determines the diffusion flux, changes insignificantly. Additionally, even at a maximum ice thickness, the thermal resistance of the ice layer is an order of magnitude lower than the resistance to heat transfer from the exhaust gas and significantly lower than the thermal resistance to heat transfer from hydrogen. These factors, combined with the change in the aggregate state of water upon reaching the triple-point temperature, explain a rapid transition from ice growth to its maximum thickness in a stationary mode. While the diffusion flow remains constant, a liquid phase is formed instead of a solid one.

The structure of the external heat fluxes is shown in Figure 5. During the ice growth phase, the diffusion heat flux exceeds the convective one. However, when the interphase surface temperature reaches the ice melting point, this heat flux decreases due to the reduction in the heat of phase transition by the heat of fusion. Under fixed heat exchange conditions, no further increase in ice thickness or decrease in diffusion heat flux occurs.

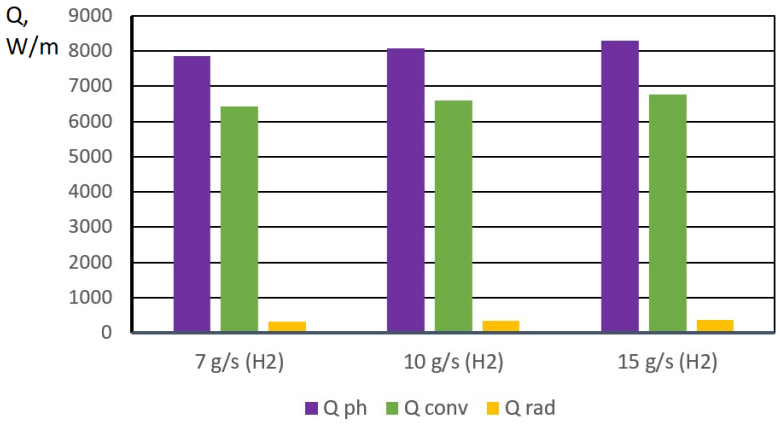


Figure 5. Structure of linear heat flux. Q ph—heat flux due to mass transfer; Q conv—heat flux due to convection; Q rad—heat flux due to radiation. Hydrogen T = 40 K, P = 20 bar; exhaust gas T = 665 K.

4. Conclusions

During icing, two opposite effects influence heat transfer. Ice formation increases the overall thermal resistance, while the phase change in the diffusing component increases the overall heat flux. Under the conditions studied in this article, the contribution of the second effect is significantly higher. From the heat exchange point of view, heat exchangers utilising a phase transition of the diffusing component are preferable. The key disadvantages of these heat exchangers include the potential of ice breaking off and a slight increase in inertance due to ice melting during operation mode change.

The ice thickness is primarily reduced by factors that decrease the heat transfer coefficient from hydrogen. These factors include a decrease in hydrogen velocity due to an increased tube diameter or decreased flow rate, as well as decreases in the Prandtl and Reynolds numbers due to changes in hydrogen state parameters. The hydrogen temperature itself has a minimal effect on the ice thickness because of the temperature profile variation during heat transfer. However, this effect may become noticeable in the case of a significant decrease in the gas mixture temperature. In this case, the achievable ice thickness also changes significantly.

The developed model allows for heat transfer parameters to be calculated in steady-state and transient modes, accounting for the formation of a multi-component condensed phase on cold walls. Such an approach improves the reliability of the heat exchanger

design and accuracy in determining its characteristics during both steady and transient operation modes.

Author Contributions: Conceptualization, I.P. and O.L.; methodology, I.P. and O.L.; software, T.M. and A.K.; validation, I.P., O.L. and T.M.; formal analysis, A.K.; investigation, O.L. and T.M.; resources, O.L.; data curation, T.M.; writing—original draft preparation, O.L.; writing—review and editing, I.P.; visualization, A.K.; supervision, O.L.; project administration, O.L.; funding acquisition, I.P. All authors have read and agreed to the published version of the manuscript.

Funding: This research was funded by HORIZON-JU-Clean-Aviation project HYDEA, GA # 101102019.

Informed Consent Statement: Informed consent was obtained from all subjects involved in the study.

Data Availability Statement: The data presented in this study are available on request from the corresponding author due to confidential.

Acknowledgments: The research leading to these results has been performed in the frame of the "HYdrogen DEmonstrator for Aviation (HYDEA)" project. The research was made in the frame of HORIZON-JU-Clean-Aviation project HYDEA, GA # 101102019. DOI 10.3030/101102019.

Conflicts of Interest: The authors declare no conflicts of interest.

References

1. Prikhodko, A.A.; Alekseenko, S.V. Obledeneniye aerodinamicheskikh poverkhnostey: Metodika modelirovaniya narastaniya l'da [Icing of Aerodynamic Surfaces: Methodology for Modeling Ice Growth]. *Aviatsionno-Kosm. Tekhnika Tekhnologiya* **2015**, 35–45.
2. Xiong, H.; Wu, W.; An, Y.; Li, X.; Zhou, Z. Asymmetric Heat Transfer in Aircraft Electrothermal Anti-Icing. *Symmetry* **2023**, *15*, 599. [CrossRef]
3. Martini, F.; Ibrahim, H.; Contreras Montoya, L.T.; Rizk, P.; Ilinca, A. Turbulence Modeling of Iced Wind Turbine Airfoils. *Energies* **2022**, *15*, 8325. [CrossRef]
4. Li, R.; Zhu, G.; Zhang, D. Investigation on the Mechanism of Heat Load Reduction for the Thermal Anti-Icing System. *Energies* **2020**, *13*, 5911. [CrossRef]
5. Nigmatulin, R.I. *Osnovy mehaniki geterogennyh sred [Fundamentals of Mechanics of Heterogeneous Environments]*; Nauka: Moscow, Russia, 1978; 336p.
6. Zhao, Z.; Li, Y.; Wang, L.; Zhu, K.; Xie, F. Experimental Study on Film Condensation of Superheated Vapour on a Horizontal Tube. *Exp. Therm. Fluid Sci.* **2015**, *61*, 153–162. [CrossRef]
7. Chang, T.B.; Yeh, W.Y.; Tsai, G.L. Film Condensation on Horizontal Tube with Wall Suction Effects. *J. Mech. Sci. Technol.* **2009**, *23*, 3399–3406. [CrossRef]
8. Benteboula, S.; Dabbene, F. Modeling of Wall Condensation in the Presence of Noncondensable Light Gas. *Int. J. Heat Mass Transf.* **2020**, *151*, 119313. [CrossRef]
9. Dehbi, A.; Janasz, F.; Bell, B. Prediction of Steam Condensation in the Presence of Noncondensable Gases Using a CFD-Based Approach. *Nucl. Eng. Des.* **2013**, *258*, 199–210. [CrossRef]
10. Thomas, T.M.; Mahapatra, P.S.; Ganguly, R.; Tiwari, M.K. Atmospheric Water Vapor Condensation on Engineered Interfaces: Busting the Myths. *arXiv* **2022**, arXiv:2210.08301. [CrossRef]
11. Isachenko, V.P.; Osipova, V.A.; Sukomel, A.S. *Teploperedacha [Heat Transfer]*; Energiya: Moscow, Russia, 1975; 688p.
12. Grigorev, V.A.; Zorin, V.M. *Teplo-i Massoobmen. Teplotehnicheskij Eksperiment. Spravochnik [Heat and Mass Transfer. Heat Engineering Experiment: Handbook]*; Energoizdat: Moscow, Russia, 1982; 512p.
13. Zhao, Z.; Li, Y.; Wang, L.; Liu, Z.; Zheng, J. Flow and Heat Transfer Characteristics of Ambient Air Condensation on a Horizontal Cryogenic Tube. *Cryogenics* **2014**, *62*, 110–117. [CrossRef]
14. Zhao, Y.; Li, G.; Dang, C.; Wu, H. Research on the Thermal Performance of the Condenser in a Loop Heat Pipe Anti-Icing System. *Front. Energy Res.* **2023**, *11*, 1306563. [CrossRef]
15. Vietze, M.; Evrim, C. Development of additively manufactured cryogenic heat exchangers for hydrogen-electric aircraft propulsion. *IOP Conf. Ser. Mater. Sci. Eng.* **2024**, *1301*, 012007. [CrossRef]
16. Wilhelmsen, Ø.; Berstada, D.; Aasena, A.; Neksåa, P.; Skaugen, G. Reducing the exergy destruction in the cryogenic heat exchangers of hydrogen liquefaction processes. *Int. J. Hydrogen Energy* **2018**, *43*, 5033–5047. [CrossRef]

17. Khurmamatov, A.; Ismailov, O.; Yusupov, R.; Isamatova, J.; Aminova, G. Study of hydrodynamics of the condensation process in heat exchanger devices. In Proceedings of the 5th International Conference on Energetics, Civil and Agricultural Engineering (ICECAE 2024), Samarkand, Uzbekistan, 13–14 May 2024; Volume 497. 12p. [CrossRef]
18. Project "Tu 155". Development of a System for the Utilization of Liquid Fuel During Bench Tests of a Gas Turbine Engine Pump. 1988. Available online: https://en.wikipedia.org/wiki/Tupolev_Tu-155 (accessed on 11 December 2023).
19. Petukhov, I.I.; Shakhov, Y.V.; Syryj, V.N.; Davydov, Y.E.; Kositsyn, I.P. Jet system for utilization of liquid hydrogen during testing of a gas turbine engine pump. In *Progress. Quality. Technology: Proceedings of the Second Congress of Engine Builders of Ukraine with Foreign Participation*; KhAI: Kharkiv, Ukraine, 1997; pp. 364–369.

Disclaimer/Publisher's Note: The statements, opinions and data contained in all publications are solely those of the individual author(s) and contributor(s) and not of MDPI and/or the editor(s). MDPI and/or the editor(s) disclaim responsibility for any injury to people or property resulting from any ideas, methods, instructions or products referred to in the content.